AN ADAPTIVE BACKSTEPPING CONTROLLER FOR LOW FREQUENCY OSCILLATIONS DAMPING IMPROVEMENT OF A MULTI-MACHINE POWER SYSTEM INCLUDING UPFCS

Shahrokh SHOJAEIAN Jafar SOLTANI
Department of Electrical Engineering, Khomeinishahr Branch, Islamic Azad University
P.O.Box 84175-119, Isfahan, Iran, Phone: +989375735237, Fax: +983112305575
Email: Shojaeian@iaukhsh.ac.ir, jsoltani@iaukhsh.ac.ir

Abstract: *In this paper the low frequency oscillations damping of a multi machine power system including UPFCs is investigated by applying the Adaptive Backstepping Control (ABC) approach. Using the third order model of synchronous machine, the nonlinear state equations of the system are derived first. Then, based on ABC the supplementary excitation control inputs as well as the system parameters estimation law are designed based on the Lyapunov stability theory. Moreover considering the sixth order model of synchronous machine, simulation results are obtained for some faults. Although UPFCs effects are taken into account in dynamic simulations, but they are designed only to regulate active power of their lines and voltage magnitudes of their buses. The results show the validity and effectiveness of the proposed control approach.*

Keywords: *Low frequency oscillations, Nonlinear control, Power system stability, UPFC.*

1. Introduction

Low-frequency oscillations, related to the small-signal stability of a power system, are detrimental to the goals of maximum power transfer and power system security. Automatic voltage regulators (AVRs) help to improve the steady-state stability of power systems, but are not as useful for maintaining stability during transient conditions. The addition of power system stabilizers (PSSs) in the AVR control loop provides the means to damp these oscillations [1, 2]. The added AVRs and PSSs are designed to act upon local measurements such as bus voltage, generator shaft speed, or the rotor angle of the associated machine. This type of feedback control is useful for local and control mode oscillations, but may be unsatisfactory for inter-area oscillations.

On the other hand, the fast progress in the field of power electronics has opened new opportunities for the power industry via utilization of the controllable FACTS devices such as UPFC, TCSC and SVC as alternative means to mitigate power system oscillations [3-6]. Because of the extremely fast control action associated with FACTS-device operations, they are promising candidates for mitigation power system oscillation and improving power system steady-state performance [7, 8]. UPFC, regarded as one of the most versatile ones in the FACTS device family [9,10], has the capabilities of controlling power flow in the transmission line, improving the transient stability, mitigating system oscillation and providing voltage support. It performs this through the control of the in-phase voltage, quadrate voltage and shunts compensation due to its main control strategy [10, 12].

In the past two decades, in order to solve the low frequency oscillation problems of the modern power systems which include the FACTS devices, some authors have tried to apply the nonlinear control methods to the these systems. Adaptive backstepping control (ABC) is one of these methods, which has been used in [13-16]. No FACTS device has been taken into account in these works.

In [13] a nonlinear feedback excitation control is used in a power system with uncertainties based on the adaptive backstepping method. A Lyapunov function is applied to analysis the convergence of the power angle and speed of the generator and the active electrical power delivered by the generator with the designed controller when a large fault occurs.

In [14] an approach for combining adaptive backstepping control and optimal reduced order models to design the power system stabilizers has been proposed**.** Adaptive backstepping control and optimal reduced order models were used to design the power system stabilizers. The advantages of the proposed method are illustrated by numerical simulation of the one-machine infinite-bus power system.

In [15] an adaptive backstepping excitation control, tuned using Particle Swarm Optimization (PSO), is designed for stability enhancement of multi-machine power systems. The interconnection terms are considered as uncertain functions of electric power and its derivative whose parameters are adapted using PSO. The proposed technique is illustrated on a 50-machine-145-bus system, which shows that the designed controllers are effective in stabilizing the system under severe contingencies and perform better when compared with conventional power system stabilizers.

In [16] the design of a nonlinear variable-gain fuzzy controller for a flexible ac transmission systems (FACTS) has been presented to enhance the transient stability performance of power systems. The fuzzy controller uses a numerical consequent rule base of the Takagi–Sugeno type, which can be either linear- or nonlinear-producing control-gain variation over a very wide range. This type of fuzzy control is expected to be more robust and effective in damping electromechanical oscillations of the power systems in comparison with the conventional PI regulators used for UPFC control. Computer simulation results validate the superior performance of this controller.

The main contribution of this paper is to use ABC technique in order to damp the low frequency oscillations of a multi machine power system which includes three UPFCs. UPFCs are used to regulate steady state active power of their lines and voltage magnitudes of their output buses. A steady state regulating signal as well as a supplementary stabilizing signal are produced for the generator exciter. The supplementary stabilizing signal is generated by an adaptive backstepping controller and a steady state regulating signal is generated by a conventional PI controller. The proposed control method in this paper is very robust and stable during the system different faults and system load disturbances when the system parameters uncertainties are taken into account. The overall system is proved by the Lyapunov theory.

In this paper, the third order model of the synchronous machine is used to develop the power system nonlinear state equations first. Then considering the sixth order model of the synchronous machines some simulation results are obtained to verify the validity of the proposed approach. The static forth order Runge-Kutta method is used to solve the system nonlinear differential equations. MATLAB® code is applied in our simulations

2. Adaptive Backstepping Controller Design

2.1. Machine Model

An Adaptive Backstepping nonlinear controller is designed in order to damp the low frequency oscillations of the practical multi-machine multi-UPFC power systems. This controller is not expected to enhance the transient stability of the selected power system before the rotor single swings of the synchronous machines. One may note that the transient stability of the system can be achieved by a high performance protection system using high speed circuit breakers. That will results in choosing the proper system fault clearance. This means that for designing the Adaptive Backstepping controller there is no need to take into account the synchronous machines subtransient states. The UPFCs are used in power systems to regulate the active and reactive powers which are decided to flow in some selected transmission lines in the system steady state condition.

Based on above descriptions, the third order model of the synchronous machine is used for designing the ABC controller:

$$\begin{aligned}
&\frac{dd_i}{dt}=w_b.(w_{ri}-1)=w_b.\Delta w_{ri}\\
&\frac{d\Delta w_{ri}}{dt}=\frac{1}{2H_i}.(P_{mi}-P_{ei})=\frac{\Delta P_{ei}}{2H_i}\\
&\frac{dE'_{qi}}{dt}=\frac{1}{T'_{d0}}\left[E_{fdi}-E'_{qi}-(X_{di}-X'_{di}).I_{dri}\right]
\end{aligned} \tag{1}$$

Where P_{mi} is the ith turbine injected power, P_{ei} is the ith synchronous machine active power, E'_{qi} is ith transient induced voltage (behind the direct axis transient inductance) and E_{fdi} is the rotor excitation voltage of the ith machine.

In addition, a simple machine rotor excitation system control is used as:

$$\frac{d\Delta E_{fdsi}}{dt}=\frac{1}{T_{ai}}\left[-\Delta E_{fdsi}+K_{ai}.\Delta Vgi\right] \tag{2}$$

Where V_{gi} is the ith machine terminal voltage magnitude. K_{ai} and T_{ai} are the ith machine AVR gain and time constant, respectively.

2.2. Power System Model

A simplified UPFC model is shown in Figures 1(a) and 1(b). Where Y_u is the admittance of the transmission line containing UPFC. With reference to Fig. 1(b), the angles of UPFC injected series and shunt space vectors ($\bar{V}_{se}, \bar{I}_{sh}$) are assumed to be respectively in 90 degrees lagging and leading with respect to transmission line current ($\bar{I}_{upfc}$) and UPFC bus voltage ($\bar{V}_{upfc}$). Such assumption is necessary to

make, in order to modulate the instantaneous active power that flows in the transmission line including UPFC, with main objective of damping the low frequency oscillations of the power system in the abnormal conditions. Notice that if in Fig.1 (b), the angle of $\bar{V}_{se}$ is adjusted for a phase angle different from 90 degrees with respect to the phase angle of the $\bar{I}_{upfc}$, both the instantaneous active and reactive powers of the UPFC line are modulated, which is not necessary for the purpose described in this paper.

Referring to Fig.1 (b), when the instantaneous active power of the UPFC transmission line tends to increase, the UPFC series injected voltage ($\bar{V}_{se}$) acts as an inductive series reactance. Reversely, when the instantaneous active power of this line tends to decrease, the mentioned signal acts as a capacitive series reactance. Such behavior of signal $\bar{V}_{se}$ causes to damp the system low frequency oscillations. It is not necessary to say that at each step Δt of time, the phase angle of $\bar{I}_{upfc}$ and $\bar{V}_{upfc}$ space vectors are obtained by simulation and in practice by measurement. Having obtained these angles, the angles of the UPFC injected signals $\bar{V}_{se}$ and $\bar{I}_{sh}$ (δ_{se} and δ_{sh}) are calculated as:

$$\delta_{sh} = \angle V_{upfc} - 90° \quad \text{and} \quad \delta_{se} = \angle I_{upfc} + 90°$$

Consider a practical multi-machine multi-UPFC modern power system, numbering machines terminal buses from 1 to N, the UPFC buses from N+1 to N+M and remaining buses from N+M+1 to N+M+P. Injected currents to the last buses are zero. Y_{bus} equations of this network can be derived as:

$$\begin{bmatrix} \bar{I}_g \\ \bar{I}_u \\ 0 \end{bmatrix} = \begin{bmatrix} \bar{Y}_{gg} & \bar{Y}_{gu} & \bar{Y}_{gp} \\ \bar{Y}_{gu}^T & \bar{Y}_{uu} & \bar{Y}_{up} \\ \bar{Y}_{gp}^T & \bar{Y}_{up}^T & \bar{Y}_{pp} \end{bmatrix} \begin{bmatrix} \bar{V}_g \\ \bar{V}_u \\ \bar{V}_p \end{bmatrix} \tag{3}$$

Where vectors $\bar{I}_g$ and $\bar{I}_u$ are the machines terminals injected currents and UPFCs injected currents, into the network respectively. Vectors $\bar{V}_g$, $\bar{V}_u$, and $\bar{V}_p$ are the machines terminals voltages, UPFCs buses voltages and the last buses voltages, respectively. With reference to Fig. 2, vector $\bar{I}_u$ can be obtained as:

$$\bar{I}_u = \begin{bmatrix} \bar{I}_{sh1} + \bar{Y}_{u1}.\bar{V}_{se1} \\ -\bar{Y}_{u1}.\bar{V}_{se1} \\ \bar{I}_{sh2} + \bar{Y}_{u2}.\bar{V}_{se2} \\ ..... \\ -\bar{Y}_{uM}.\bar{V}_{seM} \end{bmatrix} \tag{4}$$

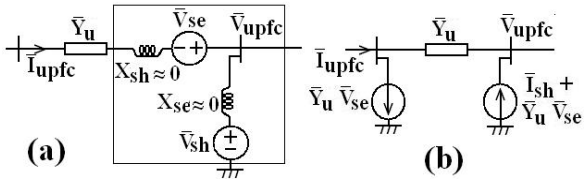

Fig. 1. UPFC Model. (a) with voltage sources (b) with current sources

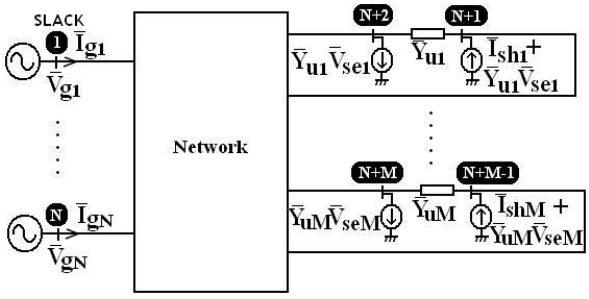

Fig. 2. Multi-machine power system used for simulation

Where $\bar{V}_{se1}$ to $\bar{V}_{seM}$ are UPFCs injected series voltages, $\bar{I}_{sh1}$ to $\bar{I}_{shM}$ are UPFCs injected shunt currents and $\bar{Y}_{u1}$ to $\bar{Y}_{uM}$ are the transmission lines admittances which include UPFCs. Using (3) and (4), one can obtain that:

$$\bar{I}_g = \left(\bar{Y}_{gg} - \begin{bmatrix} \bar{Y}_{gu} & \bar{Y}_{gp} \end{bmatrix} \begin{bmatrix} \bar{Y}_{uu} & \bar{Y}_{up} \\ \bar{Y}_{up}^T & \bar{Y}_{pp} \end{bmatrix}^{-1} \begin{bmatrix} \bar{Y}_{gu}^T \\ \bar{Y}_{gp}^T \end{bmatrix} \right) . \bar{V}_g + \begin{bmatrix} \bar{Y}_{gu} & \bar{Y}_{gp} \end{bmatrix} \begin{bmatrix} \bar{Y}_{uu} & \bar{Y}_{up} \\ \bar{Y}_{up}^T & \bar{Y}_{pp} \end{bmatrix}^{-1} \begin{bmatrix} \bar{I}_{2M} \\ \bar{0}_{P2M} \end{bmatrix} . \bar{I}_u \tag{5}$$

Where I_{2M} is a (2M×2M) unity matrix and 0_{P2M} is a (P×2M) zero matrix. Defining:

$$\bar{U} = \begin{bmatrix} \bar{I}_{sh1} & \bar{V}_{se1} & \bar{I}_{sh2} & ..... & \bar{V}_{se3} \end{bmatrix}^T \tag{6}$$

$$\bar{Y}_f = diag(\bar{Y}_{fi}) \quad and \quad \bar{Y}_{fi} = \begin{bmatrix} \bar{Y}_{ui} & 1 \\ -\bar{Y}_{ui} & 0 \end{bmatrix} \tag{7}$$

From (4) :

$$\bar{U} = \bar{Y}_f . \bar{I}_u \tag{8}$$

Combining (5) and (8) gives:

$$\bar{I}_g = \bar{Y} . \bar{V}_g + \bar{D} . \bar{U} \tag{9}$$

Where:

$$\bar{Y} = \bar{G} + j\bar{B} = \left(\bar{Y}_{gg} - \begin{bmatrix} \bar{Y}_{gu} & \bar{Y}_{gp} \end{bmatrix} \begin{bmatrix} \bar{Y}_{uu} & \bar{Y}_{up} \\ \bar{Y}_{up}^T & \bar{Y}_{pp} \end{bmatrix}^{-1} \begin{bmatrix} \bar{Y}_{gu}^T \\ \bar{Y}_{gp}^T \end{bmatrix} \right) \tag{10}$$

$$\bar{D} = \bar{E} + j\bar{F} = \begin{bmatrix} \bar{Y}_{gu} & \bar{Y}_{gp} \end{bmatrix} \begin{bmatrix} \bar{Y}_{uu} & \bar{Y}_{up} \\ \bar{Y}_{up}^T & \bar{Y}_{pp} \end{bmatrix}^{-1} \begin{bmatrix} \bar{I}_{2M} \\ \bar{0}_{P2M} \end{bmatrix} \bar{Y}_f \tag{11}$$

Notice that in transient state condition of the power system under consideration, the 1st machine is assumed to be as a slack machine, same as the steady state condition. Considering this assumption, the

machines sixth reduced order equations parallel with (9) are solved, in such a way that the terminal voltage of the slack machine is forced not to change from its steady state value.

As a result, at each step Δt of time, the injected current of this machine (into the network defined by $\bar{I}_{g1}$) can be calculated from (9). That is because its terminal voltage is a known constant value. Under this condition, it can be assumed that the *qe*-axis of common synchronous rotating reference frame is to be in the direction of the slack machine constant voltage vector, which rotates with nominal power system frequency.

It is not necessary to say that the rotor *q-d* axis of the slack machine also rotates with respect to common reference frame so that at each step Δt of time, the angle of rotation can be obtained by solving the mechanical state equations of this machine. Therefore, there is no need to solve the electrical state equations of the slack machine in our system simulation.

Using the vector equation (9), the ith machine injected current vector is transferred to common reference as:

$$I_{gei}-jI_{dei}=\sum_{k=1}^{N}(G_{ik}+jB_{ik}).(V_{qek}-jV_{dek}) + \sum_{m=1}^{M}(E_{im}+jF_{im}).(U_{qem}-jU_{dem}) \quad (12)$$

Transferring the ith machine injected current vector to its rotor reference frame by multiplying both sides of (12) by $e^{-j\delta i}$, gives:

$$I_{gri}-jI_{dri}=\sum_{k=1}^{N}(G_{ik}+jB_{ik}).(V_{qrk}-jV_{drk}).[\cos(d_i-d_k)-j.\sin(d_i-d_k)] + \sum_{m=1}^{M}(E_{im}+jF_{im}).U_m.[\cos(d_i-d_{um})-j.\sin(d_i-d_{um})] \quad (13)$$

Where δ_i is the rotor angle of this machine measured from *qe*-axis of the common reference frame and U_m is the magnitude of the mth component of the control vector given in (6). Using (13), one can obtain that:

$$I_{dri}=L_i+\sum_{m=1}^{M}S_{im}.U_m \quad (14)$$

Where:

$$L_i=\sum_{k=1}^{N}\{(G_{ik}.V_{qrk}+B_{ik}.V_{drk}).\sin(d_i-d_k) +(G_{ik}.V_{drk}-B_{ik}.V_{qrk}).\cos(d_i-d_k)\} \quad (15)$$

$$S_{im}=\sum_{m=1}^{M}(E_{im}\sin(d_i-d_{um})-F_{im}\cos(d_i-d_{um})).U_m \quad (16)$$

Based on synchronous machine third order model, the ith machine terminal voltage equations are:

$$V_{qri}=-R_i.I_{qri}-X'_{di}.I_{dri}+E'_{qi} \quad (17)$$

$$V_{dri}=-R_i.I_{dri}+X_{qi}.I_{qri} \quad (18)$$

Where R_i, X'_{di} and X_{qi} are the ith machine stator resistance, direct axis transient reactance and quadrature axis reactance, respectively. From (17) and (18), I_{qri} and I_{dri} can be obtained as:

$$I_{qri}=\frac{R_i}{a_i}E'_{qi}-\frac{1}{a_i}\left(R_i.V_{qri}-X'_{di}.V_{dri}\right) \quad (19)$$

$$I_{dri}=\frac{X_{qi}}{a_i}E'_{qi}-\frac{1}{a_i}\left(X_{qi}.V_{qri}+R_i.V_{dri}\right) \quad (20)$$

With:

$$a_i=R_i^2+X'_{di}.X_{qi} \quad (21)$$

Neglecting the stator copper losses, the ith machine generated active power is:

$$P_{ei}=V_{qri}.I_{qri}+V_{dri}.I_{dri} \quad (22)$$

Combining (19), (20), and (22) gives:

$$P_{ei}=b_i.E'_{qi}+g_i \quad (23)$$

Where:

$$b_i=\frac{1}{a_i}\left(X_{qi}.V_{dri}+R_i.V_{qri}\right) \quad (24)$$

$$g_i=\frac{-1}{a_i}\left[\left(R_i.V_{qri}-X'_{di}.V_{dri}\right).V_{qri} +\left(X_{qi}.V_{qri}+R_i.V_{dri}\right).V_{dri}\right] \quad (25)$$

Using (23), the third equation of (1) can be rewritten as:

$$\frac{dE'_{qi}}{dt}=\frac{1}{T'_{d0}}\left[E_{fdi}-(X_{di}-X'_{di}).L_i\right] -\frac{E'_{qi}}{T'_{d0}}-\sum_{m=1}^{M}\frac{X_{di}-X'_{di}}{T'_{d0}}.S_{im}.U_m \quad (26)$$

E_{fdi} has three different parts:

$$E_{fdi}=E_{fdoi}+\Delta E_{fdsi}+\Delta E_{fddi} \quad (27)$$

Here E_{fdoi} is the rotor steady state excitation voltage; DE_{fdsi} is the regulating signal for the steady state condition, generated by conventional PI controller. DE_{fddi} is the stabilizing signal for the transient state condition, generated by adaptive backstepping controller. The index i denotes that all these three parameters are for the ith machine. Now, (26) can be rewritten as:

$$\frac{dE'_{qi}}{dt}=A_i-\frac{1}{T'_{d0}}\Delta E_{fdsi}-\frac{1}{T'_{d0}}\Delta E_{fddi} \quad (28)$$

Where:

$$A_i=\frac{1}{T'_{d0}}\left[E_{fdoi}+\Delta E_{fdsi}-(X_{di}-X'_{di}).(L_i+\sum_{m=1}^{M}S_{im})\right]$$

Using the state equations of (1):

$$\begin{bmatrix} \frac{\Delta \dot{\delta}_i}{w_b} \\ \Delta \dot{w}_{ri} \\ \dot{E}'_{qi} \end{bmatrix} = \begin{bmatrix} \Delta w_{ri} \\ \frac{\Delta P_{ei}}{2H_i} \\ A_i - \frac{1}{T'_{d0}}.E'_{qi} \end{bmatrix} + \begin{bmatrix} 0 \\ 0 \\ 1 \end{bmatrix}.\Delta E_{fddi} \quad (29)$$

General form of (29) is rewritten as:

$$\dot{X}_i = f_i(X_i) + g_i \,.\, U_i \quad (30)$$

Where:

$$f_i(X_i) = [\Delta w_{ri} \quad \frac{\Delta P_{ei}}{2H_i} \quad A_i - \frac{1}{T'_{d0}}.E'_{qi}]^T$$

$$g_i = [0 \quad 0 \quad 1]^T \quad and \quad U_i = \Delta E_{fddi}$$

Choosing the system output variable as:

$$h_i = z_{1i} = \Delta\delta_i / w_b \quad (31)$$

Applying the Lie theory [17], gives:

$$\dot{z}_{1i} = L_{f_i} h_i + L_{g_i} h_i . U_i = \Delta w_{ri} \quad (32)$$

$$\dot{z}_{2i} = L^2_{f_i} h_i + L_{g_i} L_{f_i} h_i . U_i = \frac{\Delta P_{ei}}{2H_i} \quad (33)$$

$$\dot{z}_{2i} = L^3_{f_i} h_i + L_{g_i} L^2_{f_i} h_i . U_i = q_{oi} + q_{pi} . z_{3i} + q_i . U_i \quad (34)$$

Where:

$$q_{oi} = \frac{-1}{2H_i}\left[A_i b_i + \frac{P_{mi} - g_i}{T'_{d0}} \right] \quad (35)$$

$$q_{pi} = \frac{1}{2H_i . T'_{d0}} \quad (36)$$

$$q_{im} = \frac{-b_i}{2H_i . T'_{d0}} \quad (37)$$

Then, the new state equation set is:

$$\dot{z}_{1i} = z_{2i} \quad (38)$$

$$\dot{z}_{2i} = z_{3i} \quad (39)$$

$$\dot{z}_{3i} = q_{oi} + q_{zi} . z_{3i} + q_{ui} . U_i \quad (40)$$

3. Adaptive Backstepping Controller Design

Considering (36) with constant unknown parameters gives:

$$\dot{z}_{3i} = \hat{q}_{oi} + \hat{q}_{zi} . z_{3i} + \hat{q}_{ui} . U_i \quad (41)$$

Here the estimated values of each q is shown by $\hat{q}$. Obviously $\hat{v} = -K_i . z_{3i}$ can stabilize (37). Combining (36) and (37) results in:

$$\begin{aligned} \dot{z}_{3i} &= q_{oi} + q_{zi} . z_{3i} + q_{ui} . U_i + \hat{v} - \hat{v} \\ &= \tilde{q}_{oi} + \tilde{q}_{zi} . z_{3i} + \tilde{q}_{ui} . U_i - K_i . z_{3i} \end{aligned} \quad (42)$$

Where:

$$\tilde{q}_{oi} = q_{oi} - \hat{q}_{oi} \quad (43)$$

$$\tilde{q}_{zi} = q_{zi} - \hat{q}_{zi} \quad (44)$$

$$\tilde{q}_{ui} = q_{ui} - \hat{q}_{ui} \quad (45)$$

For the subsystem (34), virtual input j_{1i} is considered as:

$$\dot{z}_{1i} = j_{1i} \quad (46)$$

and the Lyapunov function can be candidate as:

$$V_{1i} = \frac{1}{2} z^2_{1i} \quad (47)$$

Choosing $f_{1i} = -K_i . z_{1i}$ and derivating V_{1i} with respect to the time in second, gives:

$$\dot{V}_{1i} = z_{1i} . \dot{z}_{1i} = -K_i . \dot{z}^2_{1i} \le 0 \quad (48)$$

For (34) and (35), virtual input f_{2i} is considered as:

$$\begin{cases} \dot{z}_{1i} = z_{2i} \\ \dot{z}_{2i} = f_{2i} \end{cases} \quad (49)$$

and Lyapunov function can be candidate as:

$$V_{2i} = V_{1i} + \frac{1}{2}(z_{2i} - f_{1i})^2 \quad (50)$$

Choosing $j_{2i} = -K_i . (z_{2i} + K_i . z_{1i})$:

$$\begin{aligned} \dot{V}_{2i} &= \dot{V}_{1i} + (\dot{z}_{2i} - \dot{f}_{1i})(z_{2i} - f_{1i}) \\ &= -K_i . z^2_{1i} - K_i . (z_{2i} + K_i . z_{1i})^2 \le 0 \end{aligned} \quad (51)$$

Finally for all system equations, the Lyapunov function can be candidate as:

$$\begin{aligned} V_i = V_{1i} + V_{2i} + \frac{1}{2}(z_{3i} - f_{2i})^2 + \frac{1}{2z_{oi}} \tilde{q}^2_{oi} \\ + \frac{1}{2z_{zi}} \tilde{q}^2_{zi} + \frac{1}{2z_{ui}} \tilde{q}^2_{ui} \end{aligned} \quad (52)$$

Where z_{oi}, z_{zi}, and z_{ui} are the positive estimation weighing coefficients. Derivating function V_i with respect to the time in second, gives:

$$\begin{aligned} \dot{V}_i &= \dot{V}_{1i} + \dot{V}_{2i} + (\dot{z}_{3i} - \dot{f}_{2i})(z_{3i} - f_{2i}) + \frac{\tilde{q}_{oi}\dot{\tilde{q}}_{oi}}{z_{oi}} + \frac{\tilde{q}_{zi}\dot{\tilde{q}}_{zi}}{z_{zi}} + \frac{\tilde{q}_{ui}\dot{\tilde{q}}_{ui}}{z_{ui}} \\ &= \dot{V}_{1i} + \dot{V}_{2i} + \tilde{q}_{oi}(z_{3i} + K_i . z_{2i} + \frac{\dot{\tilde{q}}_{oi}}{z_{oi}}) + \tilde{q}_{zi} . [z_{3i} . (z_{3i} + K_i . z_{2i}) + \frac{\dot{\tilde{q}}_{zi}}{z_{zi}})] \\ &+ \tilde{q}_{ui} . [U_i . (z_{3i} + K_i . z_{2i}) + \frac{\dot{\tilde{q}}_{zi}}{z_{zi}})] - Ki . (z_{3i} + K_i . z_{2i})^2 \end{aligned} \quad (53)$$

Then the system parameter estimation laws are obtained as:

$$\dot{\tilde{q}}_{oi} = -z_{oi} . (z_{3i} + K_i . z_{2i}) \quad (54)$$

$$\dot{\tilde{q}}_{zi} = -z_{zi} . z_{3i} . (z_{3i} + K_i . z_{2i}) \quad (55)$$

$$\dot{\tilde{q}}_{ui} = -z_{ui} . U_i . (z_{3i} + K_i . z_{2i}) \quad (56)$$

As a result, (48) is reduced to:

$$\begin{aligned} \dot{V}_i = -2K_i . z^2_{1i} - K_i . (z_{2i} + K_i . z_{1i})^2 \\ + K_i . (z_{3i} + K_i . z_{2i})^2 \le 0 \end{aligned} \quad (57)$$

Having obtained $\hat{q}_{oi}, \hat{q}_{zi}$ and $\hat{q}_{ui}$ from (54) to (56), U_i can be calculated from:

$$U_i = -\hat{q}^{-1}_{ui} . (\hat{q}_{oi} + \hat{q}_{zi} . z_{3i} + K_i . z_{3i}) \quad (58)$$

4. Simulation and Results

The reduced sixth order model of synchronous machine (that is obtained by ignoring the derivative terms in the stator d and q axis voltage equations with assumption of 1pu of rotor angular speed in electric radian per second for speed voltage terms of these equations) is used for power system simulations [17]. Considering (9) to (58) for any three phase symmetrical fault that occurs in the power system, the system nonlinear differential equations are solved by applying the numerical fourth order static Runge-Kutta method using MATLAB® code with a time step Δt of 10^{-4}s. Fig. (3) shows the control strategy used in simulations.

We consider the test network *IEEE 30-bus* system with six synchronous machines and three UPFCs as shown in Fig. (4). The synchronous machines specifications are given in [17].

Assuming the initial steady state condition of this network obtained by AC load flow analysis, suppose that a three phase symmetrical fault occurs at t=0s exactly at the middle of the line which connects the buses 17 and 24, clearing at t=0.2s accomplished with line interruption and reclosing at t=1.2s. According to the flowchart of Fig. (5), simulation results obtained for this fault are shown in Fig. (6) and Fig. (7) and Fig. (8).

To test the proposed control approach robustness, an initial error of +20% in the power system resistances as well as an initial error of -20% in the synchronous machines direct axis transient reactance, is considered. It can be seen that the Adaptive Backstepping controller is capable of damping the power system low frequency oscillations in spite of parameters uncertainties. In addition to these results, as a sample, machine2 estimated lumped parameters are shown in Fig.(9).

5. Conclusion

In this paper, the low frequency oscillations damping of multi-machine multi-UPFC power systems has been investigated by using the ABC approach. The Adaptive backstepping controller generates supplementary signals for all machines exciters. Control signals of all UPFCs are the magnitude of injected series voltage and injected shunt current space vectors, which both are generated by conventional PI regulators. At each step Δt of time, the phase angle of these vectors are obtained to be in 90 degrees lagging and leading respectively with respect to UPFC transmission line current and its bus voltage.

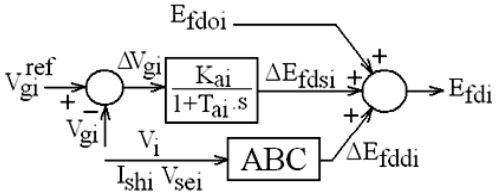

Fig. 3. Block diagram of the proposed control approach

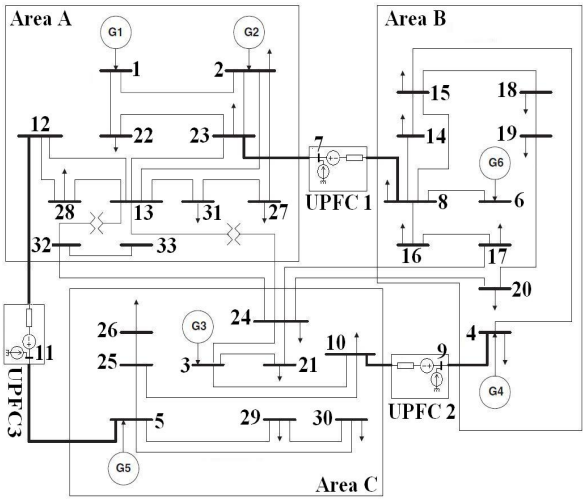

Fig. 4. Power system configuration for case study 1

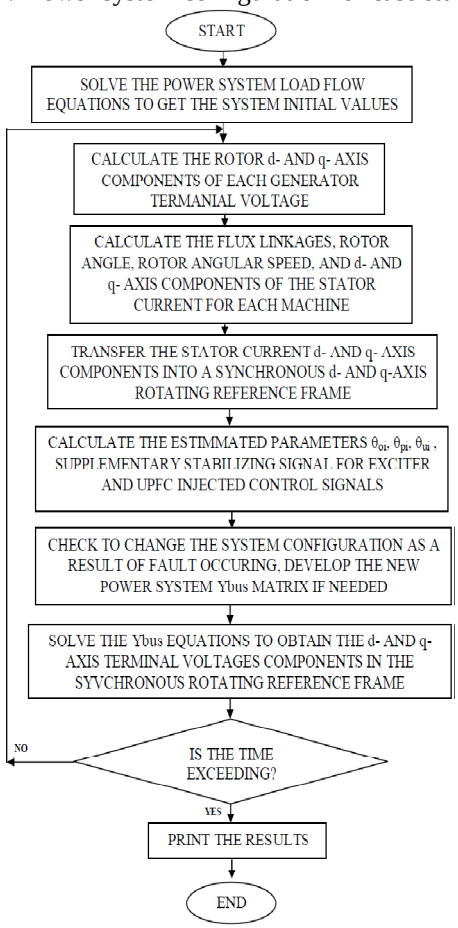

Fig. 5. Flowchart of the computer simulation program

The UPFCs have been arranged to regulate their series branch active power and output bus voltage magnitude, with reference of these parameters steady state values. Since the uncertain parameters of the power system have been chosen to be the lumped uncertain functions, therefore any number of system parameters, even all, can be assumed to be uncertain. Simulation results have been obtained for IEEE 30-bus power system with six generators and three UPFCs. A three phase symmetrical fault which accomplished with line interruption and line reclosing has been tested. These results very well support the effectiveness and capability of the proposed control approach.

6. References

[1] Abdellatif, N. : *Advanced Hybrid Control Techniques Applied on the AVR-PSS to Enhance Dynamics Performances of Electrical Networks*, In: Journal of Electrical Engineering (2011), Vol. 11, p.49-56

[2] Dysko, A., Leithead, W.E., O'Reilly, J.: *Enhanced Power System Stability by Coordinated PSS Design*,In: IEEE Transactions on Power Systems (2010), Vol.25, p. 413 - 422

[3] Anwer, N., Siddiqui, A.S., Umar, A., : *Analysis of UPFC, SSSC with and without POD in congestion management of transmission system*, In: Proceedings of India International Conference on the Power Electronics (2012), p. 6-8

[4] Kumar, N., Kumar, S., Jain, V.: *Damping sub-synchronous oscillations in power system using shunt and series connected FACTS controllers*, In: Proceedings of the International Conference on Power, Control and Embedded Systems (2010), p.1-5

[5] Mahdad B., Bouktir T., Srairi K., *The Impact Of Unified Power Flow Controller In Power Flow Regulation*, In: Journal of Electrical Engineering (2006), Vol. 6, p. 1-7

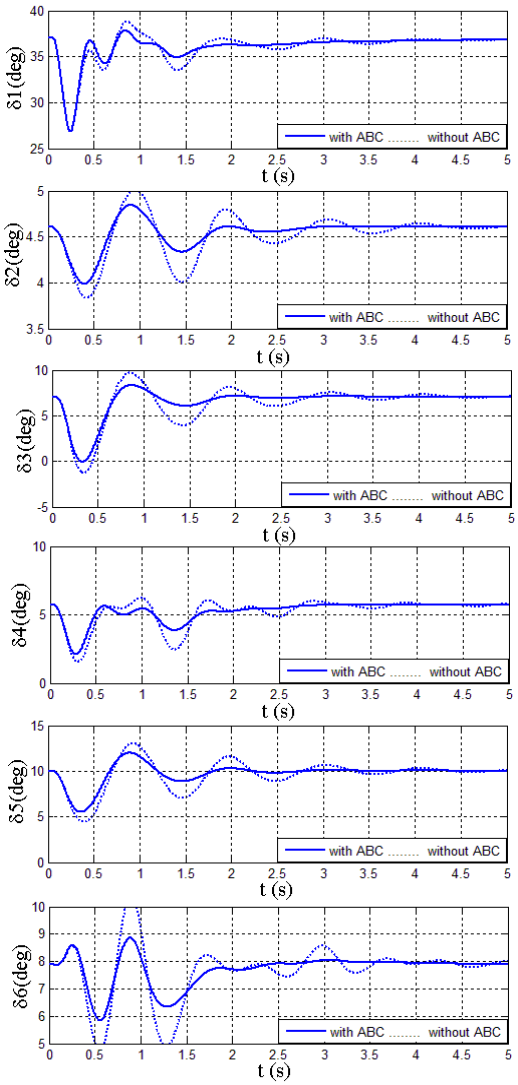

Fig. 6. Machines rotor angles with and without ABC

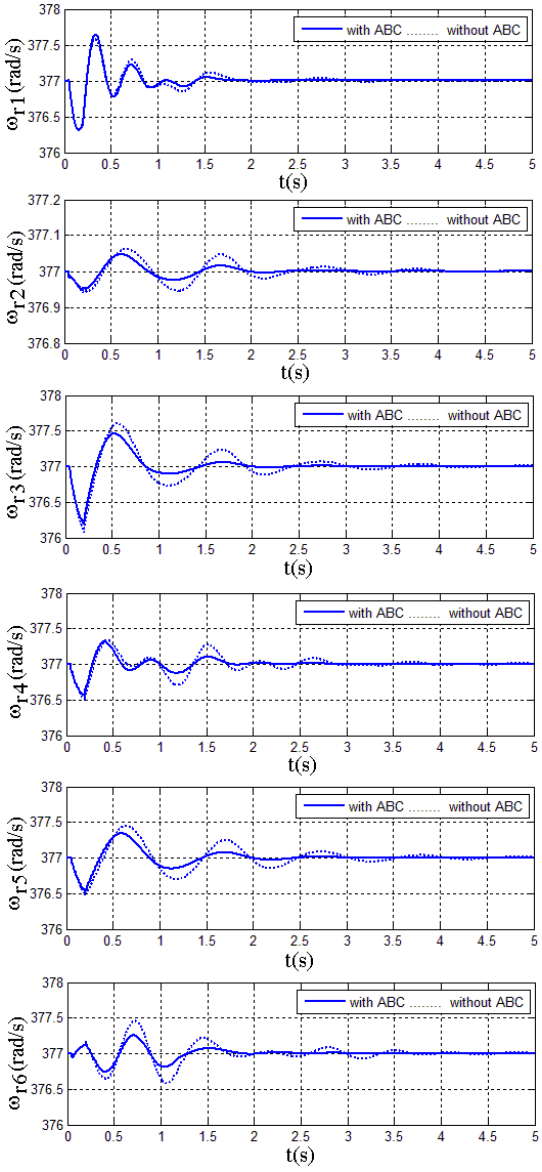

Fig. 7. Machines rotor speeds with and without ABC

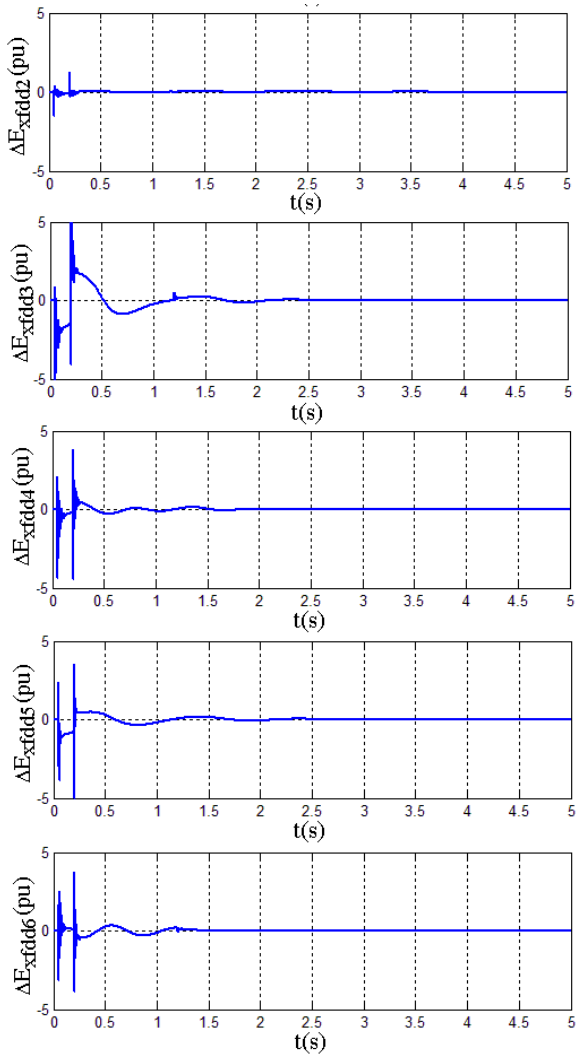

Fig. 8 Exciter Supplementary control signals generated by ABC

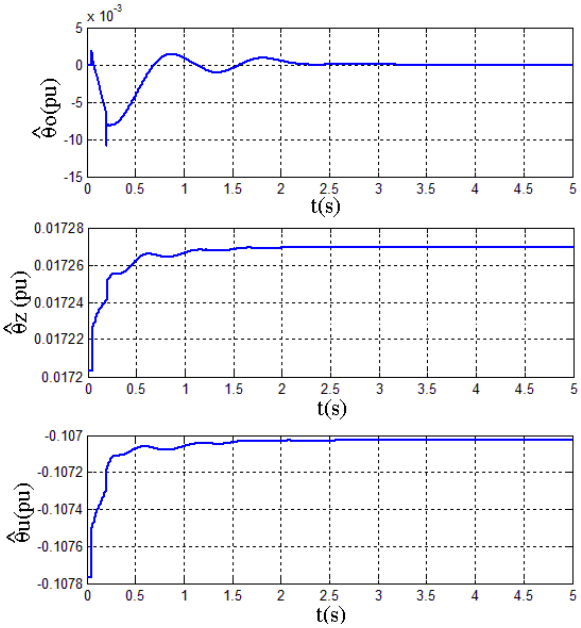

Fig. 9. Estimation of lumped uncertain functions for the synchronous machine #2

[6] Shahgholian G., Mirbagheri, S.M., Safaeipoor H., Mahdavian M. : *The effect of SVC-FACTS controller on power system oscillation damping control,* In Proceedings of the International Conference on Electrical Machines and Systems (2011), p. 20-23

[7] Sarkar M. : *Effect of UPFC allocation on transmission system power loss,* In: Proceedings of International Conference on the Energy Efficient Technologies for Sustainability (2013), p.1185,1188

[8] Merritt, N.R., Chatterjee, D.: *Performance improvement of power systems using Hybrid Power Flow Controller,* In: Proceedings of International Conference on the Power and Energy Systems (2011), p.1-6

[9] Adware, R. H., Jagtap, P. P., Helonde, J.B.: *Power System Oscillations Damping Using UPFC Damping Controller,* In: Proceedings of the International Conference on Emerging Trends in Engineering and Technology (2010), p. 340-344

[10] Al-Awami M., Abido A., Abdel-Magid Y. L.: *A PSO-based approach of power system stability enhancement with UPFC,*In: Electric Power Energy System (2007), Vol. 29, p. 251–259.

[11] Therattil J.P., Panda P.C.: *Modeling and control of a multi-machine power system with FACTS controller,* In Proceedings of International Conference the Power and Energy Systems (2011), p.1-6

[12] Talebi N. , Akbarzadeh A.: *Damping of Low Frequency Oscillations in power systems with neuro-fuzzy UPFC controller,* In: Proceedings of the International Conference on Environment and Electrical Engineering (2011), p.1-4

[13] Padiyar K. R., Uma Rao K.: *Modeling and control of unified power flow controller for transient stability,* In: Electric Power and Energy Systems (1999), Vol. 21, pp. 1–11

[14] Chang C. T., Hsu Y. Y.: *Design of UPFC controllers and supplementary damping controller for power transmission control and stability enhancement of a longitudinal power system,* In: IEE Proceedings - Generation, Transmission and Distribution (2002), Vol.149, pp. 463–471

[15] Dong L. Y., Zhang L., Crow M. L.: *A new control strategy for the unified power flow controller,* In: Proceedings of the IEEE Power Engineering Society Winter Meeting (2002), Vol. 1, p. 562–566

[16] Tan Y.L., Wang Y.: *Design of series and shunt FACTS controller using adaptive nonlinear coordinated design techniques,* In: IEEE Transactions on Power Systems (1997), Vol. 12, p. 1374–1379

[17] Shojaeian, S., Soltani, J., Markadeh, G.A., *Damping of Low Frequency Oscillations of Multi-Machine Multi-UPFC Power Systems, Based on Adaptive Input-Output Feedback Linearization Control,* In: IEEE Transactions on Power Systems (2012), Vol.27, p.1831-1840